Biosensors and Bioelectronics 90 (2017) 481–486

Contents lists available at ScienceDirect

Biosensors and Bioelectronics

journal homepage: www.elsevier.com/locate/bios

SDR-ELISA: Ultrasensitive and high-throughput nucleic acid detection based on antibody-like DNA nanostructure

Junlin Wen[a,b,c], Junhua Chen[b], Li Zhuang[b], Shungui Zhou[b,*]

[a] Guangzhou Institute of Geochemistry, Chinese Academy of Sciences, China
[b] Guangdong Key Laboratory of Agricultural Environment Pollution Integrated Control, Guangdong Institute of Eco-Environmental and Soil Sciences, Guangzhou 510650, China
[c] University of Chinese Academy of Sciences, Beijing, China

ARTICLE INFO

Keywords:
Colorimetric assay
High-throughput
Strand displacement reaction
Enzyme linked immunosorbent assay
Shewanella oneidensis

ABSTRACT

An ultrasensitive and high-throughput nucleic acid detection system, termed as strand displacement reaction-enzyme linked immunosorbent assay (SDR-ELISA), has been developed on the basis of antibody-like DNA nanostructures. Three digoxigenin or biotin modified hairpin probes are utilized to construct antibody-like DNA nanostructures that feature affinity toward streptavidin and anti-digoxigenin antibody via isothermal target-triggered SDR amplification. These antibody-like nanostructures have been employed to conjugate horseradish-peroxidase-labeled anti-digoxigenin antibody with streptavidin that is immobilized on microliter plate wells for enzyme-linked colorimetric assay. The resulting SDR-ELISA system is ultrasensitive for target DNA with a low detection limit of 5 fM. Moreover, the SDR-ELISA system is capable of discriminating DNA sequences with single base mutations, and do so in a high-throughput manner by detection and quantification of up to 96 or 384 DNA samples in a single shot. This detection system is further applied to detect other DNA targets such as *Shewanella oneidensis* specific DNA sequence, which indicates the generality of proposed SDR-ELISA system. The integration of SDR amplification and convenient ELISA technique advances an intelligent strategy for ultrasensitive and high-throughput nucleic acid detection, which may be amenable for direct visual detection and quantification using an accompanying quantitative color chart.

1. Introduction

The sensitive and convenient detection of specific nucleic acid sequences has become an important requirement in the fields of clinical diagnostics (Jung and Ellington, 2014), food safety (Kim et al., 2014; Huang et al., 2015), and environmental monitoring (Tadmor et al., 2011). Considerable efforts have been channelled toward construction of sensitive and selective DNA detection methods. Traditional southern blotting relies on complex procedures including electrophoresis, transferring and probe hybridization yet tests only for a single oligonucleotide at a time (Ferrier et al., 2015). Microarray analysis, in spite of capacity in multiplexed detection, is inherently limited by sensitivity and imperfect specificity, incapable of measuring absolute nucleic acid concentration and discriminating between closely related DNA sequences (Pritchard et al., 2012; Ferrier et al., 2015). Recently developed biosensors that utilize amplification tools such as polymerase (Chen et al., 2015), endonuclease (Yang et al., 2016), and exonuclease (Wang et al., 2015b; Chen et al., 2016), although exquisitely sensitive and selective, are frequently criticized for the strict requirements of professional laboratory conditions and sophisticated devices that result in a relatively high cost. Therefore, it is desirable to advance a facile, efficient, and economic amplification strategy for DNA detection.

Strand displacement reaction (SDR), as a popular methodology in DNA nanotechnology, has been previously proven effective for isothermal DNA amplification (Zhu et al., 2014; Li et al., 2015; Yao et al., 2015). The SDR exploits toehold (a short single-stranded overhang DNA domain) exchange mechanism (Zhang and Seelig, 2011), without the need for any enzyme or thermal annealing step, to facilitate the target-triggered assembly of metastable hairpin probes into complex DNA nanostructures, such as nanowires (Venkataraman et al., 2007), branched structures (Xuan and Hsing, 2014), nanotube (Zhang et al., 2013), tetrahedron (Sadowski et al., 2014) and hydrogel (Kahn et al., 2015). By means of toehold-mediated SDR, the initiator DNA target is released as a true catalyst and catalyzes successive cycles of assembly reaction to yield numerous DNA nanostructures, offering hundreds-fold catalytic amplification of the target hybridization event (Guo et al., 2015; Bi et al., 2016a). Due to its modularity and programmability,

* Corresponding author.
E-mail address: sgzhou@soil.gd.cn (S. Zhou).

http://dx.doi.org/10.1016/j.bios.2016.10.092
Received 10 August 2016; Received in revised form 13 October 2016; Accepted 31 October 2016
Available online 02 November 2016
0956-5663/

such SDR amplification can be further improved by encoding functional moieties, i.e. DNAzyme, digoxigenin, and biotin, into scaffold of designed DNA nanostructures (Zhang et al., 2015b; Quan et al., 2016). The feasibility of SDR to encode functional information, together with inherent modularity and enormous amplification capability, offers unique features for the transduction and amplification of analyte signal. In fact, SDR has been utilized to transduce analyte-recognizing event to various analytic modalities, including chemiluminescent (Bi et al., 2016b), photoelectrochemical (Zang et al., 2015) and electrochemical (Jia et al., 2016) assays. Despite the high sensitivity and accuracy, these analytic techniques are somewhat time-consuming and often require tedious modifications and skilled operators. In particular, the involvement of complex and expensive instruments significantly restricts their applications in resource-poor settings.

Enzyme-linked immunosorbent assay (ELISA), by contrast, is a simple yet powerful analytic technique, which can concurrently analyze up to 96 or 384 samples that contain target molecules in very small numbers. The power of ELISA originates from the exquisite Y-shaped antibodies. In this Y-shaped protein, each of the two tips (variable regions) is able to recognize one particular epitope while the base (Fc region) is able to communicate with other biological molecules (Ido et al., 2014; Rosati et al., 2014). Such versatile Y-shaped-antibody-based assay is mostly applied to detect antibiotics residues (Jiang et al., 2013), proteins (Lin et al., 2013), and antibodies (Berg et al., 2015; Li et al., 2016). However, to the best of our knowledge, ELISA has never been coupled to the isothermal SDR amplification for the detection of DNA sequences.

In this work, ELISA technique has been integrated with SDR amplification strategy for the first time to develop an ultrasensitive and high-throughput DNA detection system. This SDR-ELISA method utilizes three digoxigenin or biotin modified hairpin probes to construct antibody-like DNA nanostructures through target-catalyzed SDR amplification. The yielded antibody-like DNA nanostructures conjugate horseradish-peroxidase-labeled anti-digoxigenin antibody (HRP-Ab) with streptavidin (SA) that is immobilized on microtiter plate wells, and thus enable an enzyme-linked colorimetric assay. The integration of isothermal SDR amplification and ELISA technique offers an ultrasensitive and convenient system with a low DNA detection limit currently of 5 fM. The detection limit can be easily further reduced 2–3 orders of magnitude by switching to a fluorescent readout instead of the currently used absorbance readout. Moreover, the SDR-ELISA system is capable of discriminating DNA sequences with single base mutations, and so by detection of up to 96 or 384 DNA samples. This detection system is further applied to detect other DNA targets such as *Shewanella oneidensis* (*S. oneidensis*) specific DNA sequence, and could be extended to detect other targets by combining aptamer techniques. The developed SDR-ELISA system paves a new and cost-effective way toward analyte monitoring in a variety of fields.

2. Materials and methods

2.1. Reagents and materials

SA and precipitation-type tetramethylbenzidine (TMB) substrate solution were purchased from Sangon Biotech Co. (Shanghai, China). TMB powder was obtained from Sigma-Aldrich (St. Louis, MO). (3-aminopropyl) triethoxysilane (APTES) was provided by Aladdin (Shanghai, China). Other regents were of analytical reagent grade and used as received unless otherwise mentioned. Ultrapure water at 18.2 MΩ•cm resistivity was produced by a Milli-Q system (Millipore Corporation, Bedford, USA) and used to prepare all the solutions. The HPLC-purified oligonucleotides were synthesized by Sangon Biotech Co. (Shanghai, China) and the sequences are listed as follows. Target: 5′-GCACTACTCCCTAACATCTCAAGC-3′. DH1: 5′-GCTTGAGATG-TTAGGGAGTAGTGCTCCAATCACAACGCACTACTCCCTAACATCAAA-AA-digoxigenin-3′. DH2: 5′-AGGGAGTAGTGCGTTGTGATTGGAAA-CATCTCAAGCTC CAATCACAACGCACTAAAAAA-digoxigenin-3′. BH: 5′-GTTGTGATTGGAGCTTGAGATGTTGC ACTACTCCCTAACATCTCAAGCTCCAATAAAAA-biotin-3′.

2.2. Gel electrophoresis

Lyophilized oligonucleotide powders were dissolved in ultrapure water (nuclease-free) as stock solution, and later diluted as working solutions in phosphate buffer (50 mM Na_2HPO_4, 500 mM NaCl, pH 6.8). The solution of oligonucleotide probes DH1, DH2 and BH were respectively heated to 95 °C for 5 min, and then allowed to slowly cool to room temperature to form hairpin structures. These annealed hairpin probes were stored at 4 °C before use. To evaluate the assembly of hairpin probes, target DNA (100 nM) was mixed with the annealed probes that have a final concentration of 500 nM. The mixtures were incubated for 1 h at room temperature (RT) to yield antibody-like DNA nanostructures. After mixing with a loading buffer (V/V, 1:5), the prepared samples (5 μL per sample) were added into a 3% agarose gel in TAE buffer (40 mM Tris AcOH, 2.0 mM Na_2EDTA, pH 8.5). Gel electrophoresis was conducted at RT for 30 min under 120 V, and then photographed by using a Bio-Rad Gel Doc XR+ system (Tokyo, Japan).

2.3. Atomic force microscopy (AFM)

AFM analysis was conducted according to previous reports (Bi et al., 2015; Zhang et al., 2015a). Ten microliter of the DNA reaction mixture (100 nM) was deposited directly onto a freshly cleaved and APTES-treated mica surface, leaving to adsorb for 5 min. Next, the mica surface was washed with ultra-pure water, and dried under RT. Finally, the prepared samples were scanned with ScanAsyst-air silicon-nitride probe in ScanAsyst mode on Multimode Nanoscope-V AFM (Veeco instruments, USA), which is a mode with automatic image optimization technology.

2.4. Dot immunobinding assay

Dot immunobinding assay (Hawkes et al., 1982), an effective method for evaluating antibodies, was used to assess the immunoreactivity of antibody-like DNA nanostructures. A 0.45 μm pore-size nitrocellulose (NC) membrane was cut into circular pieces (diameter of 6 mm) using a commercial hole puncher. The circular pieces were dotted with SA diluted in phosphate-buffered saline (PBS). After drying at 37 °C, the circular NC membranes were transferred into the wells of a 96-well microplate and blocked with 3% skim milk. To each well, 100 μL of DNA reaction mixture was added. The plate was incubated overnight at 4 °C, and then subjected to three washes and 1000-fold diluted HRP-Ab solution (100 μL/well). After incubating 60 min at RT, the NC circular pieces were washed three times with PBST (PBS containing 0.5% Tween 20) and twice with PBS. The NC membranes were soaked in the precipitation-type TMB substrate solution for color development. The samples contain antibody-like DNA nanostructure would result in a purple-blue colored, insoluble substrate product developed in the NC membranes.

2.5. SDR-ELISA assay

The signal of target DNA was firstly amplified using toehold-mediated SDR. In a typical assay, 1.78 μL of each 5-μM annealed hairpin probes and 794.66 μL of phosphate buffer were mixed in a 1.5-mL tube. The prepared mixture was transferred into eight tubes, 90 μL per tube. To these tubes, 10 μL of different concentrations of target DNA samples were added to reach final concentrations of 5.0 nM, 500 pM, 50 pM, 5 pM, 500 fM, 50 fM, 5 fM and 0 fM. These samples were adequately mixed with a vortex mixer, and then allowed to react at RT for 1 h.

The products of toehold-mediated SDR were further amplified and

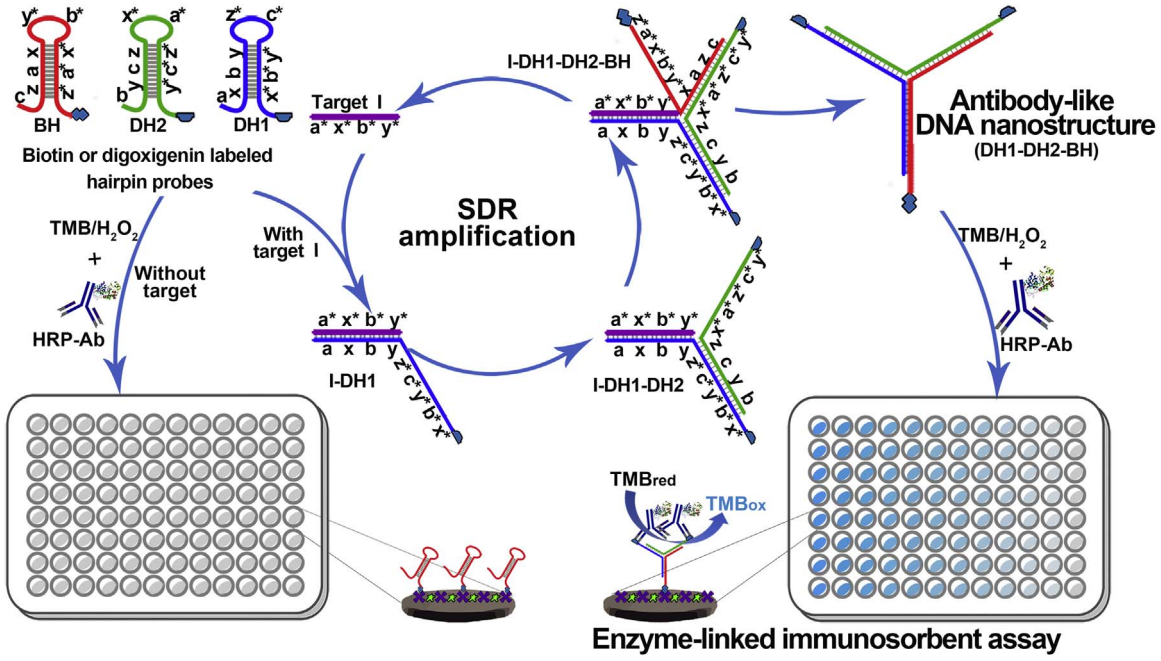

Scheme 1. Schematic illustration of SDR-ELISA system. By SDR amplification, the target signal was transduced into antibody-like DNA nanostructures which possess digoxigenin and biotin. The produced antibody-like DNA nanostructures were transferred into a microplate and thus bound to SA-coated plate via SA-biotin interaction. After removing unbound components, HRP-Ab combined with the antibody-like DNA nanostructures. The substrate TMB was converted by HRP into oxidized TMB with blue color. (For interpretation of the references to color in this figure legend, the reader is referred to the web version of this article.)

determined by using ELISA-based colorimetric assay (Wen et al., 2012). A 96-well flat-bottom polystyrene microplate (Costar, Corning, NY, USA) was pre-coated with SA and blocked with 3% skim milk. Subsequently, the reaction mixtures from the toehold-mediated SDR (100 μL per sample) were incubated in the plate for 30 min before the bound antibody-like DNA nanostructures were detected with 100 μL/well HRP-Ab diluted in 1% skim milk. After incubation for 30 min at RT, the plate was washed three times with PBST. Next, 100 μL/well TMB substrate solution (containing 100 mM citric acid, 200 mM Na_2HPO_4, 0.32 mM TMB and 2 mM H_2O_2, pH 4.3) was added and incubated for 15 min. The color development was stopped with 50 μL of 2 M H_2SO_4. Optical density at 450 nm was measured by using a Bio-rad iMark plate reader (Tokyo, Japan).

3. Results and discussion

3.1. Principle of the proposed SDR-ELISA system

The proposed SDR-ELISA system is based on toehold-mediated SDR and ELISA, of which the mechanism was illustrated in Scheme 1. Three hairpin probes (DH1, DH2 and BH) constituted of hairpin structure, digoxigenin, or biotin have been elaborately designed. The hairpin structure presented in afore-mentioned hairpin probes contains protruding toeholds (denoted **a**, **b** and **c**), and occluded toeholds (denoted **a***, **b*** and **c***) that are able to kinetically impede the formation of antibody-like DNA nanostructures in the absence of target DNA (initiator, I). When target DNA (initiator I) is introduced, however, the exposed segment **a*** of strand I nucleates at the toehold **a** of DH1, triggers a branch migration and opens the hairpin structure of DH1, and thus forms an intermediate I-DH1. In the I-DH1, toehold **b*** of DH1 functions as 'glue' to hybridize with the protruding toehold **b** of DH2, and initiates a branch migration which yields intermediate I-DH1-DH2 and exposes the toehold **c***. Upon mediation of the newly exposed toehold **c***, I-DH1-DH2 complex further hybridize with BH to form intermediate I-DH1-DH2-BH (Yin et al., 2008), which is unstable and tends to form antibody-like DNA nanostructure DH1-DH2-BH by releasing initiator strand I. The free strand I is able to successively trigger the assembly of DH1, DH2 and BH, and thus produces numerous antibody-like DNA nanostructures, which significantly amplify the signal of target DNA sequences. The as-prepared antibody-like DNA nanostructures (DH1-DH2-BH) are Y-shaded in which the tips and base are modified with digoxigenin and biotin, respectively. These bifunctional antibody-like DNA nanostructures allow the conjugation of HRP-Ab with SA-coated microplate, resulting in sandwiched HRP-Ab/DH1-DH2-BH/SA complexes that are immobilized on the wells of microplate. By employing TMB/H_2O_2 solution, these sandwiched complexes catalyze a color development, from which the blue-colored product is readily determined by using a microplate reader as well as in a facile visual observation manner.

3.2. Viability of the SDR-ELISA system

As a proof-of-concept experiment, the proposed SDR-ELISA system has been carried out using 5 nM target DNA. A characteristic blue color is observed for the target sample whereas the control (buffer containing only hairpin probes) shows no color development (inserted photo), as shown in Fig. 1. UV–vis spectra have been used to monitor the color change process. An intense absorption at 650 nm, which is the characteristic absorption of oxidized TMB from HRP-catalyzed TMB/H_2O_2 reaction (Wen et al., 2014), has been observed for the target sample. By contrast, the control sample shows no obvious characteristic absorption.

The assembly of antibody-like DNA nanostructures has been confirmed by the electrophoretogram (Fig. 1b): lane 2 shows the probe DH1; in the presence of initiator I, DH1 hybridizes with I and generates I-DH1 complex, resulting in lane 3; the complex I-DH1 reacts with probe DH2 and produces I-DH1-DH2 (lane 4); finally, the complex I-DH1-DH2 combines with BH to yield DH1-DH2-BH (lane 5). Lanes 4 and 5 correspond respectively to the intermediate and product of the assembly reaction, while lane 6 is a mixture of DH1, DH2 and BH in the absence of initiator I. The assembly of antibody-like DNA nanostructures has been further confirmed by AFM. Uniform and compact surface morphology indicates the formation of antibody-like DNA nanostructure in the presence of initiator I (Fig. 1c), whereas

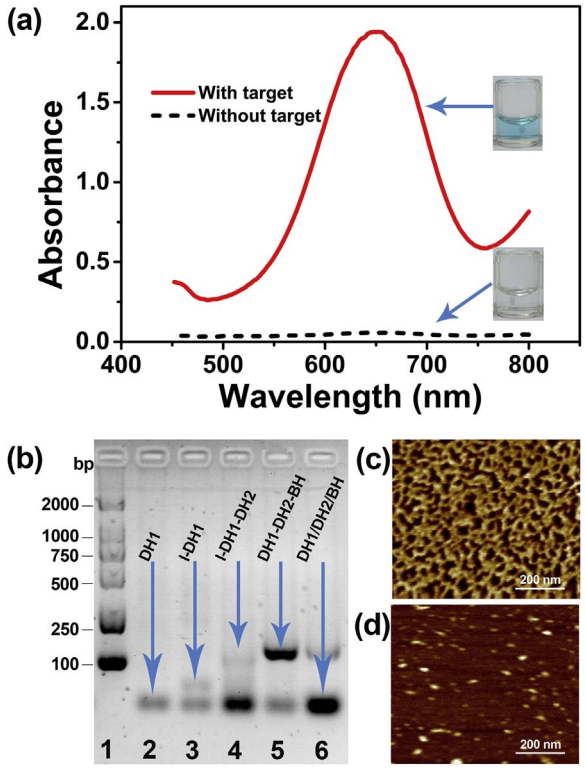

Fig. 1. Evaluation of the proposed SDR-ELISA system. (a) UV–vis spectrum of the SDR-ELISA system in the presence or absence of 5 nM target DNA. Insets are the corresponding photographs. (b) Gel electrophoresis images for the toehold-mediated SDR. Lanes: (1) DNA Ladders; (2) DH1; (3) DH1+ I; (4) DH1+ DH2+ I; (5) DH1+ DH2+ BH + I; (6) DH1+ DH2+ BH. AFM images of SDR amplification in the presence (c) or absence (d) of target DNA.

monodispersed and oval particles are observed for samples prepared in the absence of initiator I (Fig. 1d). The AFM results are in accordance with those of electrophoresis and UV–vis spectroscopy.

Furthermore, the immunoreactivity of the as-prepared antibody-like DNA nanostructures has been evaluated with dot-immunobinding assay. As shown in Fig. 2, characteristic purple-blue color of the antibody-like DNA nanostructures fades as the concentration decreases, however, the blank control containing solely hairpin probes remains colorless. These results demonstrate the immunoreactivity of antibody-like DNA nanostructures (DH1-DH2-BH).

3.3. Optimization of assay conditions

Since the toehold-mediated SDR is key to SDR-ELISA system, effect of SDR reaction time has been firstly evaluated (Fig. S1). Responsive

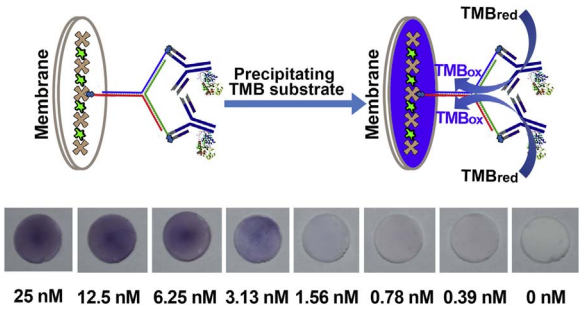

Fig. 2. Dot immunobinding assay of antibody-like DNA nanostructures. SA solution (0.1 mg/mL) was spotted on the NC membranes. Antibody-like DNA nanostructures diluted as indicated was used to conjugate HRP-Ab onto the membranes. The formed SA/DNA/HRP-Ab complex was subject to precipitating TMB substrate solution for color development. The used HRP-Ab was diluted at 1/1000.

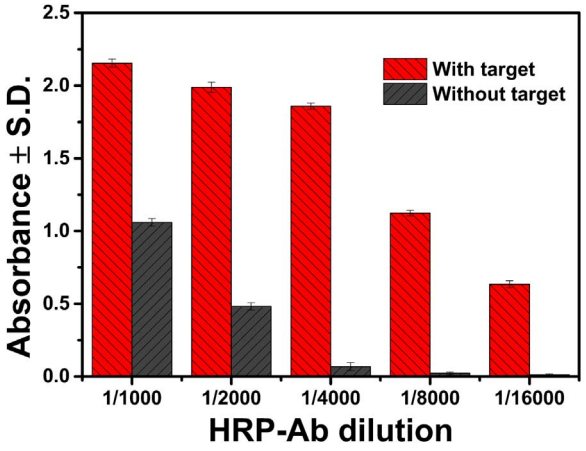

Fig. 3. Influence of HRP-Ab concentration on the response of SDR-ELISA system. HRP-Ab diluted at 1/1000, 1/2000, 1/4000, 1/8000 and 1/16000 were used in the experiment. The responsive signal was recorded in the presence or absence of 5 nM target DNA. Error bars represent the standard deviation of three independent measurements.

signals of the detection system increase continuously with reaction time, and level off gradually after 60 min. However, the background absorbance value, after increasing from 0.019 to 0.085 (from 5 to 60 min), reaches to 0.515 as SDR reaction time prolonged to 120 min. The prolonged reaction time degrades the signal-to-noise ratio and potentially affects quantitation of lower DNA concentrations, which can be attributable to the leak of kinetically controlled SDR (a spontaneous association of the hairpin probes into antibody-like DNA nanostructures). Therefore, 60 min has been selected as the optimal reaction time for SDR amplification.

The concentration of HRP-Ab, as another influence factor of TMB/HRP-based SDR-ELISA system, has been studied. Serial dilutions of HRP-Ab (ranging from 1/1000 to 1/16000) are used to evaluate the colorimetric response of SDR-ELISA system toward 5 nM target DNA. HRP-Ab diluted at 1/4000 displays better signal-to-noise ratio than those of other dilutions (Fig. 3). Lower dilution (higher concentration) of HRP-Ab significantly increases the background signal due to the nonspecific binding of HRP-Ab. Therefore, HRP-Ab diluted at 1/4000 was selected for the further experiments.

The concentration of hairpin probes is also an important factor that influences the performance of SDR-ELISA system. Responsive colorimetric signal has been enhanced as probe concentration increases from 5 to 10 nM, peaking at 10 nM, and then decreases (Fig. S2). Thus, 10 nM is considered as the optimal probe concentration for further experiments. Finally, the effect of TMB/HRP reaction time has been investigated to obtain the best assay performance. As shown in Fig. S3, the signal increases with increasing the reaction time from 5 to 15 min, then levels off. Therefore, a color developing time of 15 min is selected for the SDR-ELISA system.

3.4. Analytical performance

To assess the detection range and sensitivity of the proposed SDR-ELISA system, serial dilutions of target DNA have been analyzed under those optimized conditions. As shown in Fig. 4a, the responsive signal (absorbance at 650 nm, A_{650}) gradually grows along with target DNA concentrations. $A_{650} \pm$ S.D. (standard deviation of five independent measurements) exhibits a linear growth with a correlation coefficient of 0.98 (Fig. 4b), upon plotting against the log of target DNA concentrations. This relationship is well-described by the regression equation of $Y=0.282X+1.531$, where Y is the $A_{650} \pm$ S.D. and X is the target DNA concentrations in the range of 5 fM to 5 nM. On the basis of three times the standard deviation of the blank measurement, detection limit of the proposed method has been calculated to be 5 fM. The detection limit is

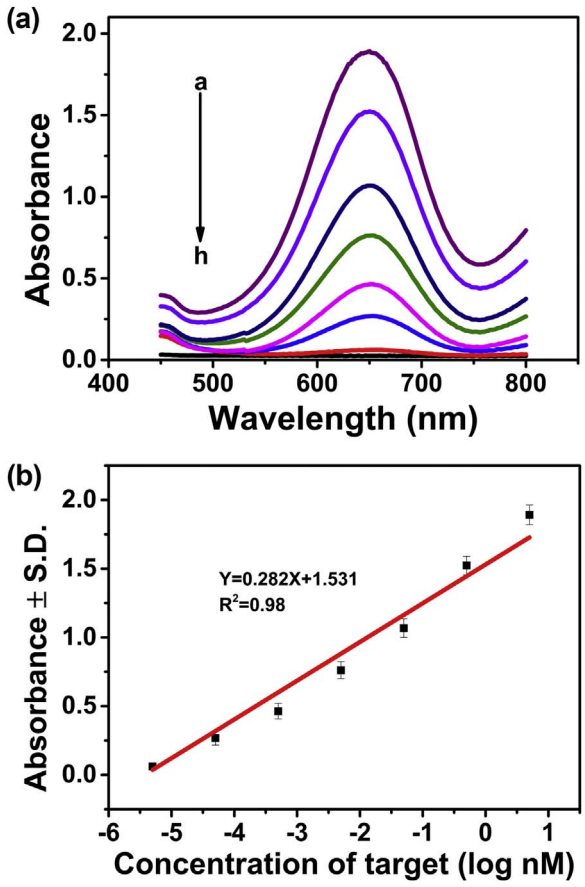

Fig. 4. Colorimetric responses of SDR-ELISA system toward various concentration of target DNA. (a) UV–vis absorption spectra of SDR-ELISA system that contain various concentration of target. (b) Plot of absorbance at 650 nm against the log of target DNA concentration. The tested DNA are 5.0 nM, 500 pM, 50 pM, 5 pM, 500 fM, 50 fM, 5 fM and 0 fM (final concentrations), curves a–h, respectively. Error bars represent the standard deviation of five independent measurements.

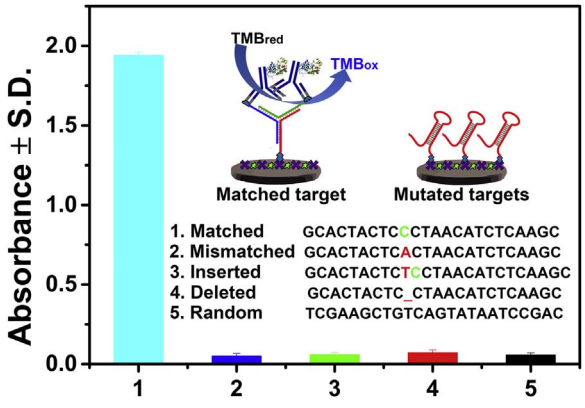

Fig. 5. Specificity of the proposed SDR-ELISA system. Mutated target DNA that is mismatched, inserted or deleted with base were determined using SDR-ELISA system. Error bars represent the standard deviation of three independent measurements.

significantly lower than that of reported methods based on SDR, including quartz crystal microbalance sensor, colorimetric assay, voltammetric method, etc. (Table S1), which demonstrates the ultra-high sensitivity of the proposed SDR-ELISA system.

3.5. Specificity and generality evaluation

Selectivity toward target DNA sequence is an important performance aspect of the proposed SDR-ELISA system. To evaluate the selectivity, the SDR-ELISA system has been challenged with target DNA sequence, target DNA sequence with mismatched, inserted and deleted base, or random DNA sequence. As shown in Fig. 5, a strong specific signal is observed in the target DNA sample, whereas there is essentially negligible signal in either mutated target DNA or noncomplementary random DNA sample. These results demonstrate the high selectivity of the proposed SDR-ELISA method toward the target DNA sequence.

On the other hand, the proposed SDR-ELISA is able to detect other DNA sequences with elaborately designed hairpin probes. The successful detection of DNA sequences specific to *S. oneidensis* (a versatile pollutant-degrading bacteria) (Marshall et al., 2006; Wen et al., 2016) have been demonstrated with novel probes DH1*/DH2*/BH and the same assay protocol (see the results and discussion in Fig. S4 of Electronic Supplementary Information). The characteristic blue color is observed in the presence of *S. oneidensis* specific target DNA. A control experiment in the absence of target DNA, no color development is discovered. This demonstrates the feasibility and generality of the proposed method in DNA detection. Furthermore, the proposed SDR-ELISA method could be extended to detect other target, upon combining with aptamer technology (Wang et al., 2015a, 2016; Xu et al., 2015), such as copper(II) ion, ampicillin residues, and platelet-derived growth factor BB. In particular, the SDR-ELISA system is compatible with automation systems thanks to its microtiter plate format (96 or 384 wells).

4. Conclusion

In summary, a novel SDR-ELISA system have been successfully developed for ultrasensitive and high-throughput nucleic acid detection based on antibody-like DNA nanostructures. The integration of efficient SDR amplification and sensitive and convenient ELISA technique has shown advantages in several aspects including isothermal amplification, ultrahigh sensitivity, high-through assay, and one base mutation discrimination. In particular, the proposed SDR-ELISA system can be extended to detect *S. oneidensis*-specific DNA sequence with newly designed hairpin probes, as well as heavy metal ions, antibiotic residues, and biomarkers by combining aptamer techniques. Furthermore, the SDR-ELISA method is also promisingly compatible with future automation systems. Overall, the proposed SDR-ELISA technology is expected to achieve technical advance and practical applications in a variety of fields.

Acknowledgements

This work was supported by the National Natural Science Foundation of China (Grant nos. 41401261, 21407029), the Guangdong Natural Science Funds for Distinguished Young Scholar (No. 2016A030306012), the Special Support Program for Young Talent Scholar of Guangdong Province (No.2015TQ01Z092), and the Science and Technology Program of Guangzhou (No. 201508020010).

Appendix A. Supplementary material

Supplementary data associated with this article can be found in the online version at http://dx.doi.org/10.1016/j.bios.2016.10.092.

References

Berg, B., Cortazar, B., Tseng, D., Ozkan, H., Feng, S., Wei, Q., Chan, R.Y.-L., Burbano, J., Farooqui, Q., Lewinski, M., 2015. ACS nano 9 (8), 7857–7866.
Bi, S., Chen, M., Jia, X., Dong, Y., Wang, Z., 2015. Angew. Chem. Int. Ed. 54 (28), 8144–8148.
Bi, S., Yue, S., Wu, Q., Ye, J., 2016a. Biosens. Bioelectron. 83, 281–286.
Bi, S., Yue, S., Wu, Q., Ye, J., 2016b. Chem. Commun. 52 (31), 5455–5458.
Chen, A., Gui, G.-F., Zhuo, Y., Chai, Y.-Q., Xiang, Y., Yuan, R., 2015. Anal. Chem. 87 (12), 6328–6334.

Chen, H.G., Ren, W., Jia, J., Feng, J., Gao, Z.F., Li, N.B., Luo, H.Q., 2016. Biosens. Bioelectron. 77, 40–45.
Ferrier, D.C., Shaver, M.P., Hands, P.J., 2015. Biosens. Bioelectron. 68, 798–810.
Guo, Y., Wu, J., Ju, H., 2015. Chem. Sci. 6 (7), 4318–4323.
Hawkes, R., Niday, E., Gordon, J., 1982. Anal. Biochem. 119 (1), 142–147.
Huang, L., Zheng, L., Chen, Y., Xue, F., Cheng, L., Adeloju, S.B., Chen, W., 2015. Biosens. Bioelectron. 66, 431–437.
Ido, S., Kimiya, H., Kobayashi, K., Kominami, H., Matsushige, K., Yamada, H., 2014. Nat. Mater. 13 (3), 264–270.
Jia, L., Shi, S., Ma, R., Jia, W., Wang, H., 2016. Biosens. Bioelectron. 80, 392–397.
Jiang, W., Wang, Z., Beier, R.C., Jiang, H., Wu, Y., Shen, J., 2013. Anal. Chem. 85 (4), 1995–1999.
Jung, C., Ellington, A.D., 2014. Acc. Chem. Res. 47 (6), 1825–1835.
Kahn, J.S., Trifonov, A., Cecconello, A., Guo, W., Fan, C., Willner, I., 2015. Nano Lett. 15 (11), 7773–7778.
Kim, T.-H., Park, J., Kim, C.-J., Cho, Y.-K., 2014. Anal. Chem. 86 (8), 3841–3848.
Li, C., Yang, Y., Wu, D., Li, T., Yin, Y., Li, G., 2016. Chem. Sci. 7 (5), 3011–3016.
Li, W., Jiang, W., Ding, Y., Wang, L., 2015. Biosens. Bioelectron. 71, 401–406.
Lin, H., Liu, Y., Huo, J., Zhang, A., Pan, Y., Bai, H., Jiao, Z., Fang, T., Wang, X., Cai, Y., 2013. Anal. Chem. 85 (13), 6228–6232.
Marshall, M.J., Beliaev, A.S., Dohnalkova, A.C., Kennedy, D.W., Shi, L., Wang, Z., Boyanov, M.I., Lai, B., Kemner, K.M., McLean, J.S., 2006. PLoS Biol. 4 (8), e268.
Pritchard, C.C., Cheng, H.H., Tewari, M., 2012. Nat. Rev. Genet. 13 (5), 358–369.
Quan, K., Huang, J., Yang, X., Yang, Y., Ying, L., Wang, H., Xie, N., Ou, M., Wang, K., 2016. Anal. Chem. 88 (11), 5857–5864.
Rosati, S., Yang, Y., Barendregt, A., Heck, A.J., 2014. Nat. Protoc. 9 (4), 967–976.
Sadowski, J.P., Calvert, C.R., Zhang, D.Y., Pierce, N.A., Yin, P., 2014. ACS nano 8 (4), 3251–3259.
Tadmor, A.D., Ottesen, E.A., Leadbetter, J.R., Phillips, R., 2011. Science 333 (6038), 58–62.
Venkataraman, S., Dirks, R.M., Rothemund, P.W., Winfree, E., Pierce, N.A., 2007. Nat. Nanotechnol. 2 (8), 490–494.
Wang, X., Dong, S., Gai, P., Duan, R., Li, F., 2016. Biosens. Bioelectron. 82, 49–54.
Wang, X., Jiang, A., Hou, T., Li, H., Li, F., 2015a. Biosens. Bioelectron. 70, 324–329.
Wang, Y., Bai, X., Wen, W., Zhang, X., Wang, S., 2015b. ACS Appl. Mat. Interfaces 7 (33), 18872–18879.
Wen, J., Chen, J., Zhuang, L., Zhou, S., 2016. Biosens. Bioelectron. 79, 656–660.
Wen, J., Zhao, S., He, D., Yang, Y., Li, Y., Zhu, S., 2012. Antivir. Res. 93 (1), 154–159.
Wen, J., Zhou, S., Chen, J., 2014. Sci. Rep. 4, 5191.
Xu, M., Gao, Z., Wei, Q., Chen, G., Tang, D., 2015. Biosens. Bioelectron. 74, 1–7.
Xuan, F., Hsing, I.-M., 2014. J. Am. Chem. Soc. 136 (28), 9810–9813.
Yang, L., Tao, Y., Yue, G., Li, R., Qiu, B., Guo, L., Lin, Z., Yang, H.-H., 2016. Anal. Chem. 88 (10), 5097–5103.
Yao, D., Song, T., Sun, X., Xiao, S., Huang, F., Liang, H., 2015. J. Am. Chem. Soc. 137 (44), 14107–14113.
Yin, P., Choi, H.M., Calvert, C.R., Pierce, N.A., 2008. Nature 451 (7176), 318–322.
Zang, Y., Lei, J., Ling, P., Ju, H., 2015. Anal. Chem. 87 (10), 5430–5436.
Zhang, C., Yang, J., Jiang, S., Liu, Y., Yan, H., 2015a. Nano Lett. 16 (1), 736–741.
Zhang, D.Y., Hariadi, R.F., Choi, H.M., Winfree, E., 2013. Nat. Commun. 4, 1965.
Zhang, D.Y., Seelig, G., 2011. Nat. Chem. 3 (2), 103–113.
Zhang, L., Guo, S., Zhu, J., Zhou, Z., Li, T., Li, J., Dong, S., Wang, E., 2015b. Anal. Chem. 87 (22), 11295–11300.
Zhu, J., Ding, Y., Liu, X., Wang, L., Jiang, W., 2014. Biosens. Bioelectron. 59, 276–281.